J. Biochem. 124, 565-571 (1998)

Isometric Contractile Properties of Single Myofibrils of Rabbit Skeletal Muscle[1]

Kiyoshi Yuri, Jun'ichi Wakayama, and Takenori Yamada[2]

Department of Physics, Faculty of Science, Science University of Tokyo, Shinjuku-ku, Tokyo 162-8601

Received for publication, March 27, 1998

The isometric contractile properties of single myofibrils of rabbit skeletal muscle were studied at various sarcomere lengths. Single myofibrils were suspended between the tips of one rigid and one flexible glass microneedle, and their force production was determined by detecting the bending of the flexible microneedle photo-electronically. The active force *vs.* sarcomere length relation had an ascending limb (0.7-2.25 μm), a plateau (2.25-2.5 μm), and a descending limb (2.5-3.8 μm), which was similar to that of frog skeletal muscle. The passive force became increasingly apparent beyond a sarcomere length of 2.4 μm. These results can reasonably be explained based on the sliding filament mechanism by assuming the sarcomere geometry of rabbit muscle. The plateau, with a produced force of about 256 kN/m^2, and the linear decline of force in the descending limb of the single myofibrils were essentially the same as those for frog muscle fibers. However, the slope of the force decline in the ascending limb was far steeper than that for frog muscle. This suggests that internal elements of sarcomeres are different between rabbit and frog muscles.

Key words: Ca^{2+}-regulation, force production, myofibril, sarcomere, skeletal muscle.

In contracting muscle, crossbridge cycling coupled with ATP hydrolysis produces force and induces the sliding of thick filaments over thin filaments (*1*). The mechanical properties of muscle have mainly been studied by use of single muscle fibers, and the ATPase reactions by use of purified actomyosin solutions. To elucidate the molecular mechanism of muscle contraction, it is essential to correlate the mechanical properties of sarcomeres of muscle fibers with the underlying biochemical reactions of the actomyosin system.

The use of single muscle fibers to study contractile properties is open to the criticism that contractions might be non-uniform, as a single fiber is composed of many bundles of myofibrils. Even in length-controlled fibers (*2, 3*), non-uniform contraction could occur at the myofibril level. Also, the limited diffusion of reactants in muscle fibers may result in non-uniform activation of the actomyosin system in skinned single muscle fibers (*4, 5*). The reaction rates of the ATP backup system may not be fast enough to yield a uniform environment of actomyosin molecules at the center and at the periphery of the muscle fiber (*6*).

Likewise, the use of purified actomyosin solutions to study biochemical reactions (*7*) has the shortcoming that the reaction mechanism in solution may not be directly applicable to the actomyosin lattice organized in muscle fibers. Similarly, the results obtained from *in vitro* motility assay to study biochemical reactions (*1*) should be applied carefully to the contractility of muscle fibers in which the actomyosin molecules are in a well-organized system (*8*).

The myofibril, which is composed of a series of sarcomeres, is the smallest contractile assembly of muscle fibers. The hexagonal lattice of actomyosin filaments in muscle fibers is well preserved in each sarcomere of myofibrils. Further, the diameter of myofibrils is small enough (*ca.* 1 μm) that the diffusion limit confronted in muscle fibers can be neglected. However experiments on myofibrils have been limited by the technical difficulty of obtaining stable single myofibril preparations for mechanical and biochemical studies. Recently, with improvements in the preparation method, several attempts have been made to study the contractile properties (*9-13*) and ATPase activities (*14-17*) of myofibrils.

In the present study, the isometric contractile properties of a single myofibril prepared from glycerinated rabbit psoas muscle have been studied, as few such data are available for rabbit muscle (*9*). The results obtained were generally similar to existing data on frog muscles and well correlated with the sarcomere structure of rabbit muscle. The results were earlier presented in preliminary form (*18*).

MATERIALS AND METHODS

Materials—Muscle fiber bundles were dissected from the psoas muscle of young New Zealand white rabbits. Fiber bundles of about 1-2 mm thickness were skinned for 30 min by immersion in a relaxing solution containing 1.0% Triton X-100 on ice. The bathing solution was then replaced with a 50% glycerol solution in 75 mM K^+-propionate, 5

[1] This work was supported by Grants-in-Aid for Scientific Research (B) (2) (No. 07458175) and (C) (2) (No. 09680658) from the Ministry of Education, Science, Sports and Culture of Japan (to T.Y.).

[2] To whom correspondence should be addressed. Tel: +81-3-3260-4271 (Ext. 2415), Fax: +81-3-5261-1023, E-mail: yamada@rs.kagu.sut.ac.jp

mM $MgCl_2$, 20 mM imidazole (pH 7.0), and the preparation was kept at 0°C overnight. After replacing the glycerol solution with a fresh one, the preparation was stored at −20°C for 5-12 weeks before use.

Myofibrils were obtained freshly before experiments. A glycerinated fiber bundle (about 1 mm in length) was cut into small pieces with scissors, suspended in 1 ml of a relaxing solution, and homogenized with a Polytron homogenizer (PT1200; Kinematica, Switzerland) at the maximal speed for 10 s on ice.

Experimental Methods—Figure 1 shows a schematic drawing of the setup for the single myofibril experiments. An experimental chamber (about 100 μl in volume) consisting of two parallel Teflon blocks attached to a glass microscope slide was installed on an inverted microscope (IMT-2; Olympus). The open ends of the chamber were sealed with silicone grease. Two glass microneedles, one rigid and one flexible, were inserted into the chamber as shown at the top of Fig. 1, each of which was connected to a micromanupilator (MO-202; Narishige). The whole assembly was supported by an air suspension table (AMF-1007; Meiritsuseiki) to minimize the effects of vibration.

After introducing a small drop of myofibril suspension into the experimental chamber, the chamber was covered with a coverslip. Then a suitable single floating myofibril was selected under the microscope, and entwined around and suspended between the tips of the two glass microneedles by the method of Anazawa *et al.* (*10*).

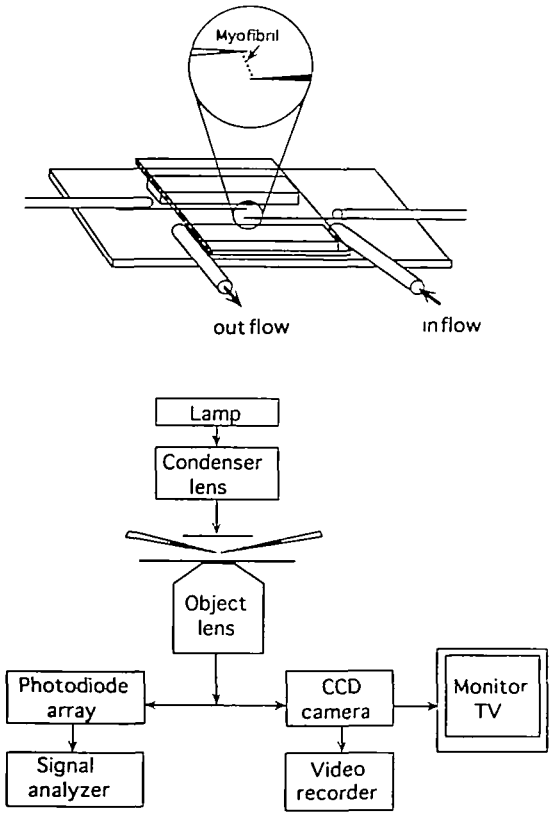

Fig. 1. **A diagram of the experimental setup and a schematic drawing of the chamber for single myofibril experiments.** In the experimental chamber shown at the top, a single myofibril preparation was suspended between the tips of two glass microneedles. The bathing solutions flowed in and out through two glass capillaries fixed at opposite ends of the experimental chamber. The whole assembly was supported by an air suspension table to minimize vibrations. See the text for details.

The bathing solution in the chamber was replaced by introducing an appropriate solution (about 500 μl) through a glass capillary fixed to one end of the chamber under gravity and withdrawing the overflow through another glass capillary fixed to the other end of the chamber with a peristaltic pump (SJ-1215; Atto). Experiments were performed at room temperature (20-24°C).

Force Measurements—The force production of single myofibril preparations was measured by detecting the bending of the flexible microneedle photo-electronically. The tip of the flexible microneedle was smeared with black oil-based ink so that a clear image could be obtained under bright illumination. The image of the tip was projected onto a photodiode linear array with 2,048 elements (OPA-2048C; Oki Electric Industry), which was mounted on an adjustable stage extending from a port of the inverted microscope. The signals of the photodiode array system were analyzed by use of a digital signal analyzer (TR9406A; Advantest) connected to a digital data recorder (TR98102; Advantest), and the position of the flexible microneedle was measured with a resolution of *ca.* 0.1 μm.

The compliance of the glass microneedles was determined by cross-bending a pair of microneedles (*19*). The elastic constants of the flexible and rigid microneedles thus determined were 0.17-0.23 and 5-7 N/m, respectively.

Sarcomere Length Measurements—The images of single myofibril preparations were continuously observed with a CCD camera (XC-77CE; Sony) through a port of the inverted microscope during measurements, and their video signals were stored in an S-VHS video cassette recorder (NV-BS900; Panasonic). The sarcomere length and the cross-sectional area of myofibrils were determined based on video images of myofibrils by use of an image processor (DVS-3000; Hamamatsu Photonix). The sarcomere striation was analyzed using computer software (NIH image; NIH) based on the video line signals scanned along the central part of the myofibril images. The single myofibril preparations suspended between the two glass microneedles were composed of 10-15 sarcomeres. As the sarcomere spacing of the preparations was uniform (< *ca.* 3% deviation), sarcomere lengths were determined as averaged values by dividing the length of a myofibril segment (generally composed of about 10 sarcomeres) by the number of sarcomere present in the segment. When preparations shortened to sarcomere lengths below 1.6 μm, their striation pattern became obscure under the optical

TABLE I. **Composition of solutions.**

	Relaxing solution	Activating solution	Contracting solution
K^+-propionate	80	70-90[a]	70
$MgCl_2$	5	5	5
$CaCl_2$	0	0.05-2.3[b]	2.3[c]
EGTA	10	2	2
Imidazole	20	20	20
ATP	5	5	5

[a]The concentration of K^+-propionate was changed to adjust the ionic strength. [b]The concentration of $CaCl_2$ was changed to obtain an appropriate free Ca^{2+} concentration. [c]The pCa of contracting solution was 4.0. The ionic strength was 150 mM. The final pH of solutions was adjusted to 7.0.

microscope. In such cases the sarcomere length was determined by dividing the length of the preparation during contraction by the number of sarcomeres observed at slack length.

Bathing Solutions—The compositions of bathing solutions are summarized in Table I. The free Ca^{2+} concentration and the total ionic strength of solutions were calculated by use of a computer program which is a modification of Fabiato and Fabiato (*20*).

RESULTS

Active Isometric Force Production of Single Myofibrils—Phase-contrasted video images of a typical single myofibril preparation suspended between the tips of a pair of microneedles are shown in Fig. 2. As described above, the preparation, 28.8 μm in length, was originally in the relaxed state (Fig. 2A). When the bathing solution was replaced with a contracting solution, the flexible microneedle deflected inward by 1.3 μm (equivalent to a force produced of 210 nN), while the rigid one did not move (Fig. 2B). The flexible microneedle returned to the original position when the bathing solution was replaced with a relaxing solution (Fig. 2C).

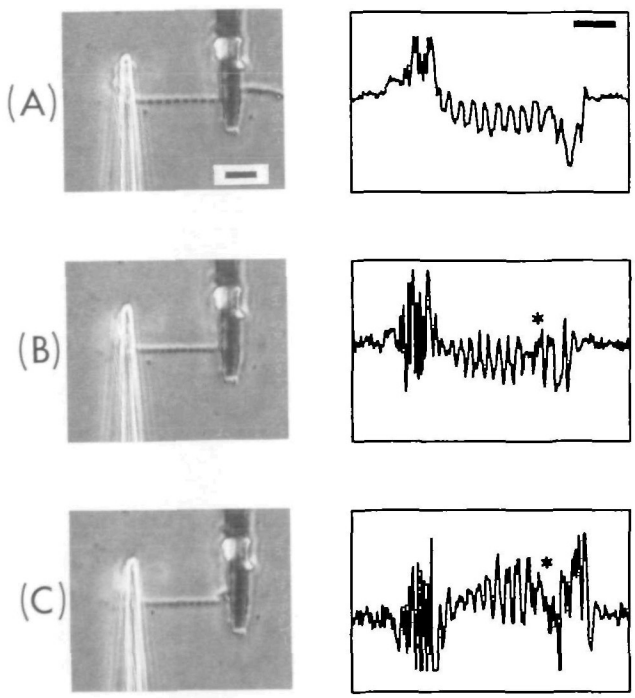

Fig. 2. **Video images of a single myofibril preparation suspended between a rigid (bright) and a flexible (dark) glass microneedle (left panels), and the corresponding intensity distributions along the central portion of the myofibril (right panels).** The (*) represents an artifact due to a myofibrillar fragment. (A) At rest, (B) during contraction, and (C) after relaxation. Each scale bar represents 10 μm.

The light intensity distributions along the video images of the myofibrils are shown in the right panels of Fig. 2. It can be seen that the original preparation is composed of nine sarcomeres with uniform striation spacing of 2.50 μm. During activation, the length of the preparation shortened slightly with the deflection of the flexible microneedle and the striation spacing decreased to 2.20 μm, while the total number of sarcomeres increased to eleven. After relaxation, the preparation returned to the original length and the striation spacing increased to 2.26 μm, while the total number of sarcomeres remained the same. Such increase in the total number of sarcomeres present in preparations was generally associated with the first contractions, possibly because the ends of preparations were more tightly entwined around the microneedles by the produced force. In the following contraction-relaxation cycles, the total number of sarcomeres in preparations stayed constant and their sarcomere spacing changed in a reversible fashion.

Figure 3 shows typical force trace produced by a single myofibril preparation associated with five consecutive contraction-relaxation cycles. It can be seen that the preparation is fully activated and relaxed within 1-2 s after exchanging the bathing solutions. The produced force in each contraction was stable, while its magnitude gradually declined in successive contractions: the forces produced in the 5th and 10th contractions respectively were *ca.* 70% and *ca.* 50% of that produced in the 1st contraction. In several experiments a pre-activating step was included prior to full activation (*21*), but it did not improve the deterioration of force production. Therefore, in the following experiments the force data obtained from the first 2-5 contractions were used for analysis.

Force-pCa Relation of Single Myofibrils at Various Sarcomere Lengths—Typical force traces produced by

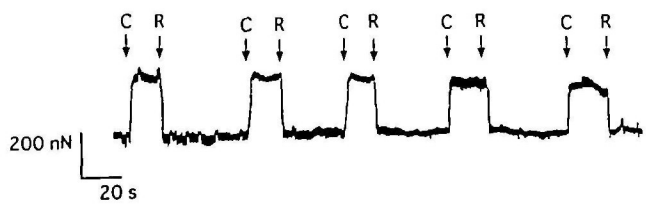

Fig. 3. **A typical force trace produced by five consecutive contraction-relaxation cycles of a single myofibril preparation at a sarcomere length of 2.4 μm.** C, contracting solution; R, relaxing solution.

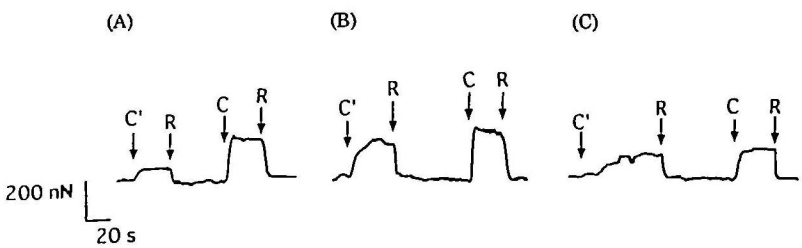

Fig. 4. **Typical force traces produced by single myofibrils activated at pCa=6.3 followed by the activation at pCa=4.0 at various sarcomere lengths.** Sarcomere length: (A) 2.1 μm, (B) 2.4 μm, and (C) 3.0 μm. C', activating solution with pCa=6.3; C, contracting solution with pCa=4.0; R, relaxing solution.

single myofibrils at sarcomere lengths of 2.1, 2.4, and 3.0 μm activated first at pCa=6.3 and then at pCa=4 are shown in Fig. 4, A-C, respectively. Similar measurements were made at each sarcomere length by changing the concentration of free Ca^{2+}. Figure 5 summarizes the relations between the active force produced by single myofibrils and the free Ca^{2+} concentration at the three sarcomere lengths. In the figure, the produced forces are normalized against that produced at pCa=4.0. It can be seen that the Ca^{2+}-sensitivity of single myofibrils at a sarcomere length of 2.4 μm increased significantly when the sarcomere length was increased to 3.0 μm, while it remained almost the same when the sarcomere length was shortened to 2.1 μm. In accord with this, the active force produced by single myofibrils at pCa=6.3 at sarcomere lengths of 2.1, 2.4, and 3.0 μm respectively was 46.3± 8.5% (mean ± SEM, n=5), 60.7±9.5% (n=8), and 85.7± 6.7% (n=7) of that produced at pCa=4.0.

Fully Activated Isometric Force Production of Single Myofibrils at Various Sarcomere Lengths—Based on the above results, we employed contracting solutions having a free Ca^{2+} concentration of pCa=4 to fully activate single myofibril preparations in the whole range of sarcomere lengths studied.

The active force production of single myofibrils at various sarcomere lengths was determined generally as follows. As preparations shortened slightly upon contraction, as shown above, their length was adjusted before each activation so as to yield an appropriate sarcomere length during contraction. To determine the force produced at sarcomere lengths greater than 2.5 μm, control force production at a sarcomere length of 2.4 μm was first measured. Second, an experimental contraction was measured at an experimental sarcomere length. Third, another control force production was measured. When the latter control force was less than 80% of the former, the data were discarded. The force produced by the two control contractions was averaged to obtain the control force. To determine the force produced at sarcomere lengths below 2.3 μm, the preparation was first activated at a sarcomere length of 2.4 μm to obtain a control force for analysis. After the preparation was fully activated, it was slowly shortened to an experimental sarcomere length and the produced force measured. Then another control force was measured. When the latter control force was less than 80% of the former, only the first control force was used for analysis.

Figure 6 shows typical force traces produced by the single myofibrils at sarcomere lengths of 1.5, 2.1, 2.4, and 3.0 μm. The magnitudes of the fully activated isometric force similarly obtained are summarized in Fig. 7 as a function of sarcomere length. Each experimental force at various sarcomere lengths was normalized against the control force at a sarcomere length of 2.4 μm. As can be seen, the fully activated force had a plateau in the sarcomere length range of 2.25-2.5 μm, the magnitude of which was 256±43 kN/m^2 (mean±SEM, n=30). As the sarcomere length was increased beyond 2.5 μm, the produced force declined linearly to zero at a sarcomere length of 3.8 μm (the descending limb). At sarcomere lengths beyond 3.8 μm, no active force was produced. As the sarcomere length was decreased below 2.25 μm, the produced force declined in a linear fashion to a sarcomere length of *ca.* 2.1 μm with a slope far greater than that of the descending limb. At a sarcomere length of *ca.* 2.1 μm, where the produced force

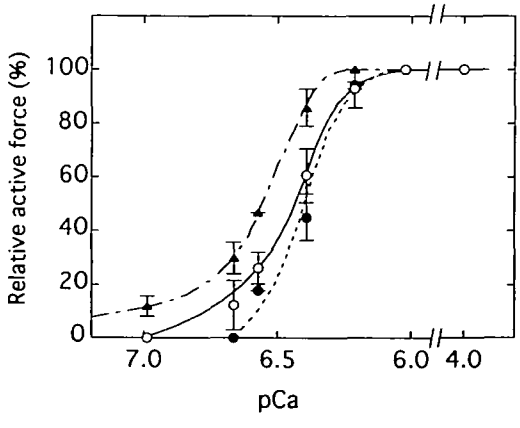

Fig. 5. **Normalized active isometric force produced by single myofibrils at various sarcomere lengths as a function of free Ca^{2+} concentration.** Sarcomere length: (●) 2.1 μm, (○) 2.4 μm, and (▲) 3.0 μm. Each data point was from 3-7 separate experiments.

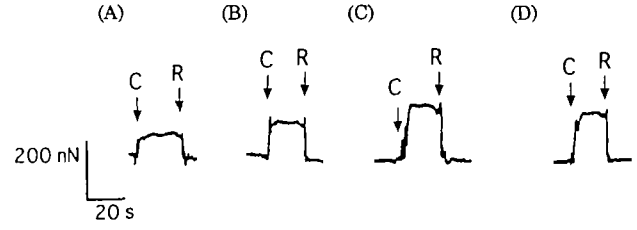

Fig. 6. **Typical force traces produced by single myofibrils activated at pCa=4.0 at four different sarcomere lengths.** Sarcomere length: (A) 1.5 μm, (B) 2.1 μm, (C) 2.4 μm, and (D) 3.0 μm. C, contracting solution; R, relaxing solution.

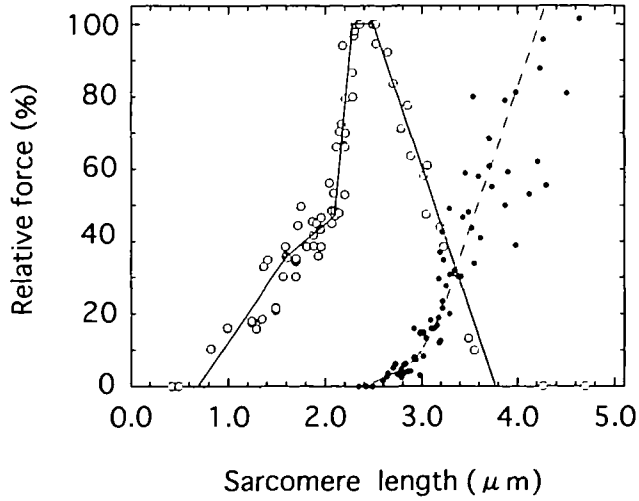

Fig. 7. **Isometric force produced by fully activated single myofibrils as a function of sarcomere length.** Included is the passive force produced by stretching relaxed single myofibrils as a function of sarcomere length. The solid line for the active force (○) and the broken line for passive force (●) were drawn by eye. Each data point was from separate experiments, although those of the active force at sarcomere lengths of 2.3-2.5 μm were from 10 to 20 separate experiments.

was *ca.* 50% of the maximal force, the force decline became less steep to a sarcomere length of *ca.* 1.6 μm. At a sarcomere length of *ca.* 1.6 μm where the produced force was about 30-40% of the maximal force, the force decline became steep again and hit zero at a sarcomere length of *ca.* 0.7 μm.

Passive Force Production of Single Myofibrils—The passive force became apparent when relaxed single myofibril preparations were stretched beyond a sarcomere length of 2.4 μm, and the force increase during the stretch was followed by gradual decay. Relaxed single myofibrils could reversibly be stretched and shortened in the sarcomere length range between *ca.* 2.2 and *ca.* 3.5 μm. However when preparations were stretched beyond a sarcomere length of 3.5 μm, the force production was impaired significantly due to damage in the sarcomere structure.

Based on this, the passive force was determined as follows. At sarcomere lengths below 3.0 μm, preparations were stretched quickly to an experimental sarcomere length and the force level was measured at 20 s after the stretch, when the force decay had nearly leveled off. Then the control active force was measured at a sarcomere length of 2.4 μm. At sarcomere lengths beyond 3.0 μm, the passive force was first measured at a sarcomere length of 3.0 μm and then at an experimental sarcomere length. Finally, the passive force at the experimental sarcomere length was determined based on that at a sarcomere length of 3.0 μm determined separately. The passive force *vs.* sarcomere length relation thus obtained is included in Fig. 7, where passive forces are expressed relative to the control active force.

DISCUSSION

As can be seen in Fig. 2, the present single myofibril preparations originally had uniform striation spacing along the whole length under the optical microscope. It was noticed, however, that the characteristic striation pattern became slightly blurred after several contraction-relaxation cycles, although the sarcomere spacing changed in a uniform and reproducible fashion. Bartoo *et al.* (*11*) reported that their single myofibril preparations developed partial damage of sarcomere structure after contractions. Although we did not observe clear damage of sarcomere striation, it is apparent from the changes in the pattern of the light intensity distribution, as can be seen in Fig. 2, that our preparations suffered local damage.

In the following, assuming possible local damage to sarcomeres does not significantly affect the overall contractilities of the myofibril, we will try to correlate the obtained results with the sarcomere structure composed of a lattice of thick and thin filaments with interconnecting filaments. The dimensions of relevant structural elements in the sarcomere of rabbit psoas muscle were assumed as follows: length of thin filaments (from tips to the center of the Z-line) = 1.12 μm (*22*); length of thick filaments = 1.63 μm (*22*); width of Z-line = 0.07 μm (*23*); width of bare zone = 0.16 μm (*24*). As can be seen in Fig. 8, there are critical stages of sarcomere lengths as follows: contact of the tips of thin and thick filaments, 3.87 μm; full overlap between thin filaments and crossbridges in the near half of thick filaments, 2.24-2.40 μm; contact between the tips of the two thin filaments extending from opposite Z-lines [and collision of the tips of thin filaments with the M-line (*25*)], 2.24 μm; contact between the tips of thin filaments and crossbridges in the far half of thick filaments, 2.08 μm; collision between the tips of thick filaments and Z-lines, 1.70 μm; collision between the tips of thin filaments and the opposite Z-lines, 1.15 μm.

Passive Force Production of Single Myofibrils—As preparations were in a relaxed state, damage to the sarcomere structure may be minimal during passive force measurement. The passive force *vs.* sarcomere length relationship for single myofibrils shown in Fig. 7 quantitatively agrees with that reported for chemically skinned single skeletal muscle fibers (*26, 27*) and for single skeletal myofibrils (*11*).

It is generally believed that the passive force is exclusively produced by an elastic protein called connectin (*28*) [or titin (*29*)] which connects the tips of thick filaments with the Z-line. In accord with this, the passive force *vs.* sarcomere length curve of single myofibrils is very similar to that of single connectin molecules (*30*) and well correlated with the sarcomere structure of rabbit muscle.

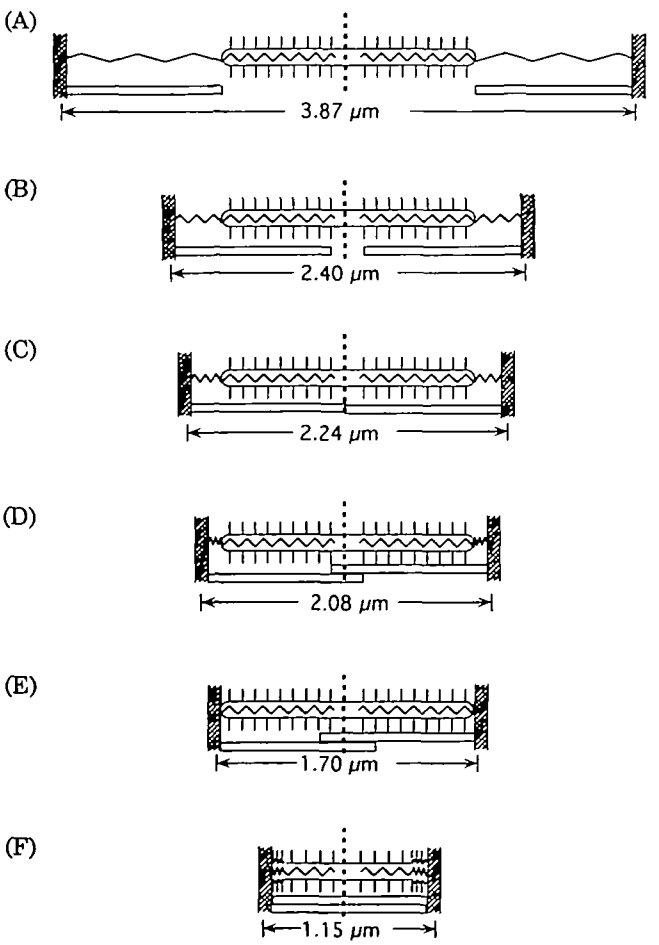

Fig. 8. Schematic drawings of the sarcomere structure at the critical sarcomere lengths. In (A)-(F), the dimensions of relevant structural elements are assumed as follows: length of thin filament (from tips to the center of Z- line), 1.12 μm; length of thick filament, 1.63 μm; width of Z- line, 0.07 μm; width of bare zone, 0.16 μm. The dotted line in the center of each figure represents the M-line. See the text for details.

Active Force vs. Sarcomere Length Relationship of Single Myofibrils—The force *vs.* sarcomere length relations for single muscle fibers have been studied in detail in frog muscle but, as far as we know, very few results are available for mammalian muscle (*9, 31*). Contractilities of rabbit muscle, for example, have generally been analyzed by assuming the force-sarcomere length relation obtained for frog muscle based on the sarcomere geometry of rabbit muscle. The active force *vs.* sarcomere length relation of the present single myofibrils shown in Fig. 7 is composed of an ascending limb in the sarcomere length range of 0.7-2.25 μm, a plateau in the sarcomere length range of 2.25-2.5 μm, and a descending limb in the sarcomere length range of 2.5-3.8 μm. This is similar to that obtained for frog muscle (*2*).

The magnitude of the maximal tension produced in the plateau, 256 kN/m^2, is nearly equal to those reported for single myofibrils (*11, 12*) and for single fiber preparations (*32, 33*) under similar conditions.

The present single myofibril preparations developed active force in a similar fashion in the descending limb as well as in the plateau, as can typically be seen in Fig. 6D. Therefore the produced force can be determined directly. On the other hand, it is known that the produced force in stretched single fibers gradually increases, and this increase is called "creep" (*2*). The produced force at that sarcomere length can be determined only after correcting for the "creep" by assuming that it is an artifact due to the progressive development of irregular sarcomere spacing (*2*). The force traces of the present single myofibril preparations suggest that the sarcomere spacing remained practically uniform during contraction at stretched lengths. Further, as can be seen in Fig. 7, the descending limb starts suddenly at a sarcomere length of around 2.5 μm and decreases linearly to zero at a sarcomere length of around 3.8 μm. Such a sharp onset and linear decline of the descending limb, which have not been observed in other muscle fiber preparations, again indicate that the sarcomere structure remained practically intact and the preparations were uniformly activated. Friedman and Goldman (*12*) reported that the myofibril bundles with longer initial sarcomere lengths developed a non-uniform striation pattern during force development. The difference between this result and ours might be due to smaller number of sarcomeres in the present single myofibril preparations.

It should be remarked that the slope of the ascending limb of the present single myofibrils shown in Fig. 7 is strikingly steeper than that of frog muscle (*2*). The force drop in the ascending limb indicates that some elements of the underlying sarcomere structure impose structural constraints against further shortening. Therefore, the difference in the ascending limb profile may suggest a difference in the internal elements of sarcomere structure between frog and rabbit muscles. Based on Fig. 8, the possible elements may be (i) the filament overlap between neighboring thin filaments, (ii) M-line component, or (iii) the thin filaments with a dense region adjacent to the Z-line (*34*). It can also be noted that the force decline became less steep at a sarcomere length slightly below 2.1 μm. This could be explained by an additional contractile force produced by the interaction of the thin filament with crossbridges having reversed polarity in the far side of the thick filament (*35*). At a sarcomere length of 1.6 μm, where the tips of thick filaments collide with the Z-line, the force decline became steep again. The net force produced by the actomyosin system eventually became zero (at sarcomere lengths of *ca.* 0.7 μm) due to the compression of thick filaments against the Z-line. As there seems to be no bend in the slope due to the collision of the tips of thin filaments with the Z-line, this may not produce appreciable resistive force against sliding. Thus the obtained force *vs.* sarcomere length relation of single myofibrils correlates well with the sarcomere structure of rabbit muscle shown in Fig. 8.

Sugi *et al.* (*9*) reported that the ascending limb was absent in single myofibril bundles: the plateau extended from 2.5 μm down to *ca.* 1.4 μm. To clarify the difference between this finding and the present results, we investigated force production in single myofibrils by lowering the temperature, using myofibrils differently prepared, or including a pre-activation step. However, we could not reproduce their results and do not know the reason for the difference.

Ca^{2+}-Sensitivity of the Active Force Production of Single Myofibrils at Various Sarcomere Lengths—As can be seen in Fig. 5, the Ca^{2+}-sensitivity of single myofibrils increased as the sarcomere length was increased from 2.4 to 3.0 μm. This is in accord with the results of skinned single fibers (*36*). On the other hand, the Ca^{2+}-sensitivity did not change significantly as the sarcomere length was decreased from 2.4 to 2.1 μm. Considering the overlap between the thin and thick filaments at the three sarcomere lengths based on Fig. 8, the above results suggest that the Ca^{2+}-sensitivity of the active force production by the actomyosin lattice in muscle changes depending on the extent of the overlap between the thin and thick filaments.

Thus the force *vs.* sarcomere length relation of the present single myofibril preparations well correlated with the sarcomere structure of rabbit muscle. In the plateau and the descending limb, it was essentially the same as that of frog muscle (*2*), considering the difference in the dimensions of sarcomere elements between frog and rabbit muscles. However, the great difference in the ascending limb between rabbit and frog muscles indicates that some internal sarcomere elements are different depending on the animal species. In conclusion the present study showed that, by use of single myofibrils, we can study contractilities of muscle without the difficulties confronted in single muscle fibers as described in the introduction.

The authors are indebted to Dr. K. Oiwa, Kansai Advanced Research Center, Communications Research Laboratory, Kobe, for his kind instruction in glass microneedle techniques and other technical supports; Dr. S. Ishiwata, Waseda University, Tokyo, for his kind instruction in the method of myofibril manipulation for mechanical measurement; and Dr. J.M. Squire, Imperial College, London, for his kind instruction in the detailed sarcomere geometry of rabbit psoas muscle and for stimulating discussions.

REFERENCES

1. Bagshaw, C.R. (1993) *Muscle Contraction*, Chapman & Hall, London, UK
2. Gordon, A.M., Huxley, A.F., and Julian, F.J. (1966) The variation in isometric tension with sarcomere length in vertebrate muscle fibres. *J. Physiol.* **184**, 176-192
3. Edman, K.A.P. and Raggiani, C. (1987) The sarcomere length-tension relation determined in short segments of intact muscle fibres of the frog. *J. Physiol.* **385**, 709-732

4. Hellam, D.C. and Podolsky, R.J. (1969) Force measurements in skinned muscle fibers. *J. Physiol.* **200**, 807-819
5. Elzinga, G., Steinern, G.J., and Wilson, M.G. (1989) Isometric force production before and after chemical skinning in isolated muscle fibres of the frog *Rana temporaria*. *J. Physiol.* **410**, 171-185
6. Pate, E. and Cooke, R. (1989) Addition of phosphate to active muscle fibers probes actomyosin states within the powerstroke. *Pflugers Arch.* **414**, 73-81
7. Lymn, R.W. and Taylor, E.W. (1971) Mechanism of adenosine triphosphate hydrolysis by actomyosin. *Biochemistry* **10**, 4617-4624
8. Homsher, E., Wang, F., and Sellers, J.R. (1992) Factors affecting movement of F-actin filaments propelled by skeletal muscle heavy meromyosin. *Am. J. Physiol.* **262**, C714-C723
9. Sugi, H., Ohta, T., and Tameyasu, T. (1983) Development of the maximum isometric force at short sarcomere lengths in calcium-activated muscle myofibrils. *Experientia* **39**, 147-148
10. Anazawa, T., Yasuda, K., and Ishiwata, S. (1992) Spontaneous oscillation of tension and sarcomere length in skeletal myofibrils. *Biophys. J.* **61**, 1099-1108
11. Bartoo, M.L., Popov, V.I., Fearn, L.A., and Pollack, G.H. (1993) Active tension generation in isolated skeletal myofibrils. *J. Muscle Res. Cell Motil.* **14**, 498-510
12. Friedman, A.L. and Goldman, Y.E. (1996) Mechanical characterization of skeletal muscle myofibrils. *Biophys. J.* **71**, 2774-2785
13. Colomo, F., Piroddi, N., Poggesi, C., te Kronnie, G., and Tesi, C. (1997) Active and passive forces of isolated myofibrils from cardiac and fast skeletal muscle of the frog. *J. Physiol.* **500**, 535-548
14. Ohno, T. and Kodama, T. (1991) Kinetics of adenosine triphosphate hydrolysis by shortening myofibrils from rabbit psoas muscle. *J. Physiol.* **441**, 685-702
15. Ma, Y. and Taylor, E.W. (1994) Kinetic mechanism of myofibril ATPase. *Biophys. J.* **66**, 1542-1553
16. Herrmann, C.C., Lionne, R., Travers, R., and Barman, T. (1994) Correlation of actoS1, myofibrillar, and muscle fiber ATPases. *Biochemistry* **33**, 4148-4154
17. Houadjeto, M., Barman, T., and Travers, F. (1991) What is the true ATPase activity of contracting myofibrils? *FEBS Lett.* **281**, 105-107
18. Yamada, T. and Yuri, K. (1996) Contractile properties of single myofibrils of skeletal and heart muscles. *Prog. Biophys. Mol. Biol.* **65**, 173
19. Yoneda, M. (1960) Force exerted by a single cilium of *Mytilus edulis* I. *J. Exp. Biol.* **37**, 461-468
20. Fabiato, A. and Fabiato, F. (1979) Calculator programs for computing the composition of the solutions containing multiple metals and ligands used for experiments in skinned muscle cells. *J. Physiol. (Paris)* **75**, 463-505
21. Moisescu, D.G. (1976) Kinetics of reaction of calcium-activated skinned muscle fibres. *Nature* **262**, 610-613
22. Sosa, H., Popp, D., Ouyang, G., and Huxley, H.E. (1994) Ultrastructure of skeletal muscle fibers studied by a plunge quick freezing method: myofilament lengths. *Biophys. J.* **67**, 283-292
23. Schachat, F.H., Canine, A.C., Briggs, M.M., and Reedy, M.C. (1985) The presence of two skeletal muscle α-actinins correlates with troponin-tropomyosin expression and Z-line width. *J. Cell Biol.* **101**, 1001-1008
24. Craig, R. (1977) Structure of A-segments from frog and rabbit skeletal muscle. *J. Mol. Biol.* **109**, 69-81
25. Luther, P.K., Munro, P.M.G., and Squire, J.M. (1981) Three-dimensional structure of the vertebrate muscle A-band. III. M-region structure and myosin filament symmetry. *J. Mol. Biol.* **151**, 703-730
26. Horowitz, R. (1992) Passive force generation and titin isoforms in mammalian skeletal muscle. *Biophys. J.* **61**, 392-398
27. Salvati, G., Betto, R., Ceoldo, S., and Pierobon-Bormioli, S. (1990) Morphological and functional characterization of the endosarcomeric elastic filament. *Am. J. Physiol. (Cell Physiol.* **28**) **259**, C144-C149
28. Maruyama, K., Matsubara, S., Natori, R., Nonomura, Y., Kimura, S., Ohashi, K., Murakami, F., Honda, S., and Eguchi, G. (1977) Connectin, an elastic protein of muscle. Characterization and function. *J. Biochem.* **82**, 317-337
29. Wang, K., Ramirez-Mitchell, R., and Palter, D. (1984) Titin is an extraordinary long, flexible and slender myofibrillar protein. *Proc. Natl. Acad. Sci. USA* **81**, 3685-3689
30. Rief, M., Gautel, M., Oesterhelt, F., Fernandez, J.M., and Gaub, H.E. (1997) Reversible unfolding of individual titin immunoglobulin domains by AFM. *Science* **276**, 1109-1112
31. Stephenson, D.G. and Williams, D.A. (1982) Effects of sarcomere length on the force-pCa relation in fast- and slow-twitch skinned muscle fibres from the rat. *J. Physiol.* **333**, 637-653
32. Dantzig, J.A., Hibberd, M.G., Trentham, D.R., and Goldman, Y.E. (1991) Cross-bridge kinetics in the presence of MgADP investigated by photolysis of caged ATP in rabbit psoas muscle fibres. *J. Physiol.* **432**, 639-680
33. Higuchi, H. and Goldman, Y.E. (1991) Sliding distance between actin and myosin filaments per ATP molecule hydrolyzed in skinned muscle fibres. *Nature* **352**, 352-354
34. Hirose, K. and Wakabayashi, T. (1988) Thin filaments of rabbit skeletal muscle are in helical register. *J. Mol. Biol.* **204**, 797-801
35. Yamada, A. and Wakabayashi, T. (1993) Movement of actin away from the center of reconstituted rabbit myosin filament is slower than in the opposite direction. *Biophys. J.* **64**, 565-569
36. Endo, M. (1972) Stretch-induced increase in activation of skinned muscle fibres by calcium. *Nature* **237**, 211-213